

A Novel Method for Measurement of Submembrane ATP Concentration*

Received for publication, February 8, 2000, and in revised form, May 8, 2000
Published, JBC Papers in Press, June 23, 2000, DOI 10.1074/jbc.M001010200

Fiona M. Gribble^{‡§}, Gildas Loussouarn[¶], Stephen J. Tucker^{‡**}, Chao Zhao[‡], Colin G. Nichols[¶],
and Frances M. Ashcroft^{‡ ‡‡}

From the [‡]University Laboratory of Physiology, Oxford University, Parks Road, Oxford OX1 3PT, United Kingdom and
the [¶]Department of Cell Biology and Physiology, Washington University School of Medicine, St. Louis, Missouri 63110

There has been considerable debate as to whether adenosine triphosphate (ATP) is compartmentalized within cells and, in particular, whether the ATP concentration directly beneath the plasma membrane, experienced by membrane proteins, is the same as that of the bulk cytoplasm. This issue has been difficult to address because there is no indicator of cytosolic ATP, such as those available for Ca^{2+} , capable of resolving the submembrane ATP concentration ($[\text{ATP}]_{\text{sm}}$) in real time within a single cell. We show here that mutant ATP-sensitive K^+ channels can be used to measure $[\text{ATP}]_{\text{sm}}$ by comparing the increase in current amplitude on patch excision with the ATP dose-response curve. In *Xenopus* oocytes, $[\text{ATP}]_{\text{sm}}$ was 4.6 ± 0.3 mM ($n = 29$) under resting conditions, slightly higher than that measured for the bulk cytoplasm (2.3 mM). In mammalian (COSm6) cells, $[\text{ATP}]_{\text{sm}}$ was slightly lower and averaged 1.4 ± 0.1 mM ($n = 66$). Metabolic poisoning (10 min of 3 mM azide) produced a significant fall in $[\text{ATP}]_{\text{sm}}$ in both types of cells: to 1.2 ± 0.1 mM ($n = 24$) in oocytes and 0.8 ± 0.11 mM for COSm6 cells. We conclude that $[\text{ATP}]_{\text{sm}}$ lies in the low millimolar range and that there is no gradient between bulk cytosolic and submembrane [ATP].

ATP-sensitive potassium channels (K_{ATP} channels) couple cell metabolism to electrical activity and play important roles in the physiology and pathophysiology of many tissues (1). In pancreatic β -cells these channels couple changes in blood glucose concentration to insulin secretion. In cardiac tissue they are involved in action potential shortening during ischemia, and in vascular smooth muscle they regulate vessel tone. Although K_{ATP} channels are inhibited by intracellular ATP with a K_i of ~ 10 μM in excised patches, substantial channel activity is observed in intact β -cells under conditions where measured cytosolic [ATP] is 3–5 mM. It has therefore been proposed that the submembrane ATP concentration ($[\text{ATP}]_{\text{sm}}$)¹ may be lower than that of the bulk cytoplasm (1, 2). A similar suggestion has

been made for liver cells under conditions of metabolic inhibition (3, 4). By contrast, studies of the Na/K-ATPase in erythrocytes have suggested that $[\text{ATP}]_{\text{sm}}$ may actually be higher than that of the bulk cytosol (4, 5). Resolution of this issue requires a method for measuring $[\text{ATP}]_{\text{sm}}$.

One way to measure $[\text{ATP}]_{\text{sm}}$ would be to use an ATP-sensitive channel as a biosensor, in the same way that Ca^{2+} -activated K^+ channels have been used to monitor submembrane $[\text{Ca}^{2+}]_i$ (6). The wild-type K_{ATP} channel is not suitable for this purpose because in intact cells the inhibitory effect of ATP is partially masked by an additional stimulatory action of MgADP (7, 8). However, the K_{ATP} channel is an octamer of two subunits: Kir6.2 and SUR (9, 10). Kir6.2 is an inwardly rectifying potassium channel pore that is intrinsically sensitive to ATP, whereas SUR endows Kir6.2 with sensitivity to the stimulatory effects of MgADP (11–14). Although wild-type K_{ATP} channels require both subunits for functional activity, a mutant form of Kir6.2 with a C-terminal truncation of 26 or 36 amino acids (Kir6.2 ΔC) is capable of independent functional expression (14). This channel is inhibited by ATP but is not activated by MgADP, making it a potential tool for monitoring $[\text{ATP}]_{\text{sm}}$.

In this paper, we show that Kir6.2 ΔC can be used as a biosensor for measurement of $[\text{ATP}]_{\text{sm}}$. We found that in *Xenopus* oocytes $[\text{ATP}]_{\text{sm}}$ was ~ 5 mM under resting conditions, whereas in mammalian cells, $[\text{ATP}]_{\text{sm}}$ averaged around 1 mM. Metabolic poisoning produced a significant fall in $[\text{ATP}]_{\text{sm}}$ in both types of cells. Thus, $[\text{ATP}]_{\text{sm}}$ is similar to or greater than the average $[\text{ATP}]_{\text{cyt}}$ and submembrane ATP gradients are unlikely to contribute to the metabolic regulation of K_{ATP} channel activity.

EXPERIMENTAL PROCEDURES

Oocyte Experiments—A C-terminal truncation of 26 or 36 amino acids of mouse Kir6.2 (GenBankTM accession number D50581) was made by the introduction of a stop codon at the appropriate residue by site-directed mutagenesis. There was no difference in the ATP sensitivity of mutants carrying a 26- or 36-amino acid truncation (14), so they are simply referred to here as Kir6.2 ΔC , for simplicity. Site-directed mutations in Kir6.2 ΔC were made using the pALTER vector. Synthesis of mRNA encoding wild-type and mutant mouse Kir6.2 was carried out as described previously (15).

Xenopus oocytes were defolliculated and injected with ~ 2 ng of mRNA encoding either wild-type or mutated Kir6.2 ΔC , or Kir1.1a. The final injection volume was ~ 50 nl/oocyte. Isolated oocytes were maintained in tissue culture and studied 1–4 days after injection (15). Whole-cell currents were measured at 18–24 °C using a standard 2-electrode voltage clamp (14) in (mM): 90 KCl, 1 MgCl₂, 1.8 CaCl₂, 5 HEPES (pH 7.4 with KOH). The holding potential was -10 mV. Currents were filtered at 1 kHz, digitized at 4 kHz, and measured 280–295 ms after the start of the voltage pulse.

Macroscopic currents were recorded from giant inside-out patches at a holding potential of 0 mV and at 18–24 °C (15). The pipette solution contained (mM): 140 KCl, 1.2 MgCl₂, 2.6 CaCl₂, 10 HEPES (pH 7.4 with KOH). The internal (bath) solution contained (mM): 110 KCl, 1.4 MgCl₂, 30 KOH, 10 EGTA, 10 HEPES (pH 7.2 with KOH), and nucleotides as indicated. Macroscopic currents were recorded in response to

* This work was supported by the Wellcome Trust and by National Institutes of Health Grant HL45742 (to C. G. N.). The costs of publication of this article were defrayed in part by the payment of page charges. This article must therefore be hereby marked "advertisement" in accordance with 18 U.S.C. Section 1734 solely to indicate this fact.

§ Recipient of a Wellcome Trust Advanced Fellowship for Medical Graduates.

¶ Recipient of a fellowship from the American Heart Foundation (Missouri affiliate).

** Recipient of a Wellcome Trust Career Development Award.

‡‡ To whom correspondence should be addressed: University Laboratory of Physiology, Oxford University, Parks Rd., Oxford OX1 3PT, UK. Tel.: 01865-272478; Fax: 01865-272469; E-mail: frances.ashcroft@physiol.ox.ac.uk.

¹ The abbreviations used are: $[\text{ATP}]_{\text{sm}}$, submembrane ATP concentration; Ap_4A , diadenosine polyphosphate.

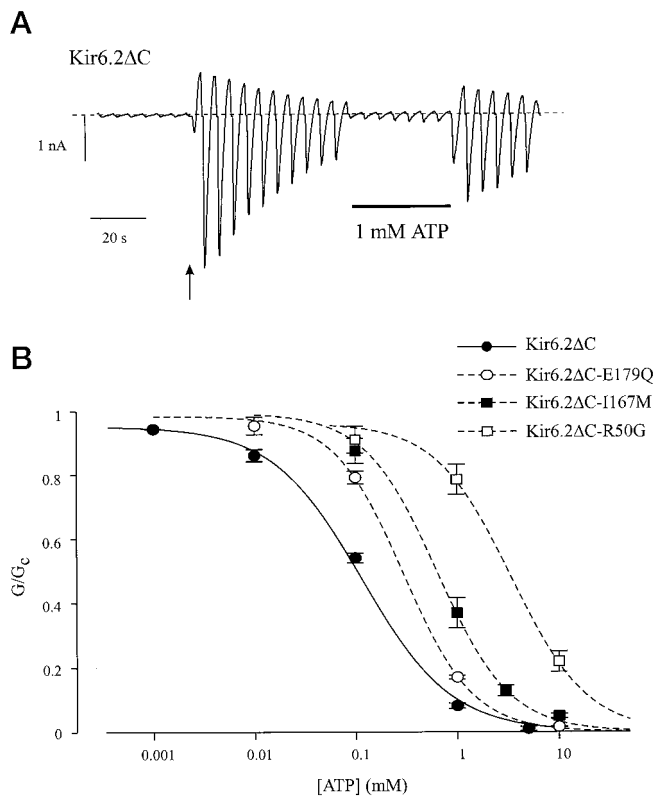


FIG. 1. *A*, macroscopic currents recorded from a giant patch on an oocyte injected with Kir6.2 Δ C. The holding potential was 0 mV, and the voltage was successively ramped from -110 to $+100$ mV over a 3-s period. The patch was excised into ATP-free solution at the arrow. 1 mM ATP was subsequently added to the intracellular solution as indicated. *B*, mean dose-response relationships for wild-type Kir6.2 Δ C ($n = 11$) and for Kir6.2 Δ C-I167M ($n = 5$), Kir6.2 Δ C-R50G ($n = 6$), and Kir6.2 Δ C-E179Q ($n = 7$). The slope conductance (G) is given as a fraction of the mean conductance (G_c) obtained in control solution before and after exposure to ATP. The lines are the best fit to the Hill equation to the data using the mean values for K_i , given in the text.

3-s voltage ramps from -110 to $+100$ mV, filtered at 0.2 kHz, and sampled at 0.5 kHz. The slope conductance was measured by fitting a straight line to the data between -20 and -100 mV; the average of five consecutive ramps was calculated in each solution, except when the currents were measured immediately after patch excision, when only 2 ramps were averaged to avoid errors due to channel rundown. Currents were corrected for leak ($<1\%$ of the total current) by subtraction of the mean current recorded in Kir6.2 Δ C-injected oocytes at a maximally effective concentration of ATP.

COSm6 Cell Experiments—Mouse Kir6.2 and hamster SUR1 (GenBankTM accession number L40623) were used for these experiments. Point mutations were made in a Kir6.2 Δ C36-C166S construct (Kir6.2 Δ CS), in which the C terminus was truncated by 36 amino acids and cysteine 166 was replaced by serine. Mutations were prepared by overlap extension at the junctions of relevant residues using the sequential polymerase chain reaction (16), and the resulting polymerase chain reaction products were subcloned into the pCMV6b vector for transfection. In some experiments, we used a mutant form of SUR1 in which glycine 1485 was replaced by aspartic acid (abbreviated here as SUR1-GD).

COSm6 cells (a variety of COS cells) were plated at a density of $\sim 2.5 \times 10^5$ cells per well in 30-mm 6-well dishes and cultured in Dulbecco's modified Eagle's medium plus 10 mM glucose supplemented with fetal calf serum (10%), penicillin (100 units/ml), and streptomycin (100 mg/ml). The next day, cells were transfected with pCMV6b-Kir6.2 Δ CS (with mutations as described), pECE-SUR1-GD, and pGreenLantern (Life Technologies, Inc.) using LipofectAMINE reagent (Life Technologies, Inc.) according to the manufacturer's instructions. Currents were recorded at -50 mV from cell-attached and inside-out patches from green fluorescent cells using a chamber that allowed rapid solution changes (16). Current amplitudes were measured by fitting a straight line through the data points once the current had reached a steady state. Both bath (intracellular) and pipette (extracellular) solu-

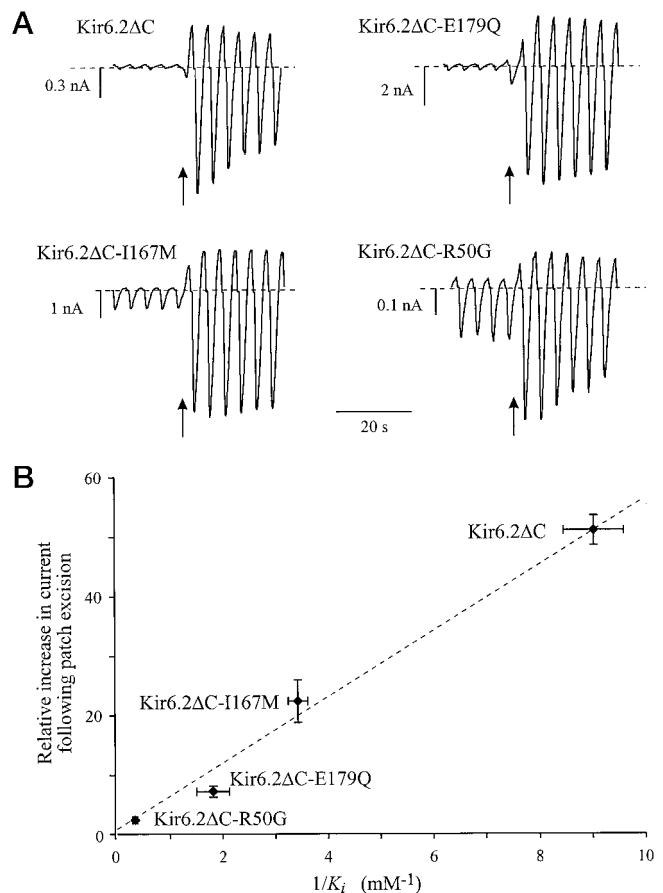


FIG. 2. *A*, macroscopic currents recorded from four different patches in response to a series of voltage ramps from -110 to $+100$ mV. Oocytes were injected with mRNAs encoding Kir6.2 Δ C, Kir6.2 Δ C-E179Q, Kir6.2 Δ C-E167M, or Kir6.2 Δ C-R50G. The patch was excised into ATP-free solution at the arrows. The dashed line indicates the zero current level. *B*, relationship between the increase in conductance on patch excision and $1/K_i$ for channel inhibition by ATP for the channels indicated. The conductance following excision is expressed as a fraction of that in the cell-attached configuration. The line is drawn to the equation $G/G_c = 1/(1 + ([ATP]/K_i)^h)$ with $h = 1.0$ and the concentration of ATP = 5.7 mM.

tions contained (mM): 140 KCl, 1 K-EGTA, 10 K-HEPES (pH 7.3), with additions as described.

Data Analysis—All data are given as mean \pm S.E. The symbols in the figures indicate the mean, and the vertical bars indicate one S.E. (where this is larger than the symbol). ATP dose-response relationships were fit to the Hill equation: $G/G_c = 1/(1 + ([ATP]/K_i)^h)$, where G is the slope conductance in the presence of ATP, G_c is the mean conductance obtained in control solution (before and after ATP application), $[ATP]$ is the ATP concentration, K_i is the ATP concentration at which inhibition is half-maximal, and h is the slope factor (Hill coefficient). Statistical significance was tested using Student's t test.

RESULTS

Oocyte Experiments—Currents recorded from cell-attached patches on oocytes injected with Kir6.2 Δ C were very small but increased ~ 50 -fold following patch excision (Fig. 1*A*). This increase in conductance was not observed in water-injected oocytes, indicating that it results from activation of Kir6.2 Δ C currents that are inhibited in the cell-attached configuration. Subsequent application of 1 mM ATP to the intracellular membrane surface largely blocked Kir6.2 Δ C currents, suggesting that the submembrane ATP concentration may be responsible for channel inhibition in the intact oocyte. Consistent with this idea, large currents were recorded from cell-attached patches on oocytes expressing the ATP-insensitive Kir channel Kir1.1 α , and no change in conductance was observed on patch excision. The mean Kir1.1 α conductance was 15.0 ± 3.6 nanosiemens in

TABLE I
Estimation of $[ATP]_{sm}$ from the increase in conductance following patch excision

[ATP] was calculated from $[ATP] = (G_2/G_1 - 1)^{1/h} \times K_i$, where G_1 is the slope conductance in the cell-attached condition, G_2 is the slope conductance immediately after excision of the same patch, K_i is the concentration of ATP required to block the channel half-maximally, and h is the Hill coefficient for the dose-response curve for ATP inhibition.

Oocytes					
Clone	G_1	G_2	G_2/G_1	$[ATP]_{sm}$	n
<i>nanosiemens</i>					
<i>mM</i>					
Kir6.2ΔC	0.56 ± 0.05	28 ± 2	51 ± 2	5.8 ± 0.3	9
Kir6.2ΔC-E179Q	2.2 ± 0.7	41 ± 9	22 ± 4	5.0 ± 0.8	8
Kir6.2ΔC-I167M	2.6 ± 0.8	16.4 ± 4.4	7.2 ± 0.9	3.2 ± 0.5	8
Kir6.2ΔC-R50G	2.3 ± 0.7	5.8 ± 1.9	2.4 ± 0.2	4.2 ± 0.5	4
COSm6 cells					
Clone	G_2/G_1	$[ATP]_{sm}$			
<i>mM</i>					
Kir6.2ΔCS-I154C	0.15 ± 0.06	1.8 ± 0.6	4		
Kir6.2ΔCS + SUR1-GD	0.47 ± 0.06	0.96 ± 0.14	29		
Kir6.2ΔCS-I154C + SUR1-GD	0.12 ± 0.04	1.4 ± 0.3	14		
Kir6.2ΔCS-T171C + SUR1-GD	0.65 ± 0.10	1.83 ± 0.28	19		

the cell-attached patch and 15.5 ± 3.9 nanosiemens after patch excision ($n = 5$, data not shown). The mean conductance in control (water-injected) oocytes was <0.2 nanosiemens.

A critical test of whether the amplitude of Kir6.2ΔC currents in the intact cell reflects $[ATP]_{sm}$ is to examine mutant channels with altered ATP sensitivity, because these should produce markedly different current amplitudes in cell-attached patches yet yield similar values of $[ATP]_{sm}$. We studied three different Kir6.2ΔC mutations that reduce the channel ATP sensitivity to differing extents: R50G, I167M, and E179Q (Fig. 1B). Half-maximal inhibition (K_i) of wild-type Kir6.2ΔC currents was produced by $115 \pm 6 \mu\text{M}$ ATP ($n = 11$). Mutation of the arginine at position 50 to glycine (R50G) reduced the K_i for ATP inhibition to 3.4 mM, mutation of isoleucine 167 to methionine (I167M) decreased the K_i to 640 μM , and mutation of glutamate 179 to glutamine (E179Q) reduced the K_i to 300 μM (17). As expected, channels that showed lower ATP sensitivity exhibited larger currents in the cell-attached configuration and a smaller increase in conductance on patch excision (Fig. 2A and Table I). There was a reciprocal relationship between the K_i for current inhibition by ATP and the increase in conductance on patch excision (Fig. 2B), and the $[ATP]_{sm}$ calculated from each set of data was similar (see Fig. 4 and Table I). This constitutes good evidence that the principal cytosolic regulator of Kir6.2ΔC activity is $[ATP]_{sm}$. The mean value of the submembrane ATP concentration in oocytes calculated from all the data given in Table I (and Fig. 2) is 4.6 ± 0.3 mM ($n = 29$) and that from the slope of the graph in Fig. 2B is 5.7 mM.

Mammalian Cell Experiments—We also measured the submembrane ATP concentration in mammalian cells using a similar approach with another C-terminally deleted construct of Kir6.2 (Kir6.2ΔCS-I154C). This contains the double mutation C166S and I154C, which shifts the ATP sensitivity of the channel into the appropriate physiological range: $K_i = 0.54 \pm 0.12$ mM ($n = 4$). Table I shows that the estimated $[ATP]_{sm}$ in COSm6 cells using Kir6.2ΔCS-I154C was 1.8 ± 0.6 mM. The patch current level in such experiments was generally quite low. As reported previously (14), the level of current is enhanced by coexpression of SUR1. To obtain larger patch currents, and hence increase the accuracy of measured channel activities, we performed further experiments on cells coexpressing Kir6.2ΔCS constructs with a mutant SUR1 containing the point mutation G1485D (SUR1-GD). This mutation abolishes nucleotide diphosphate stimulation of K_{ATP} channel cur-

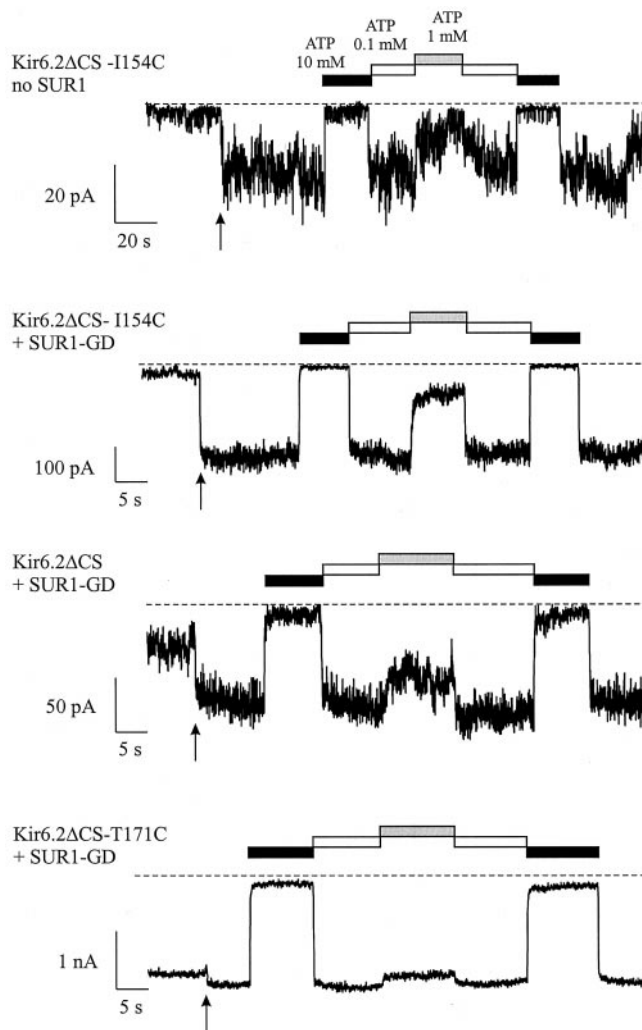


FIG. 3. Macroscopic currents recorded from four different membrane patches on COSm6 cells transfected with Kir6.2ΔCS-I154C, Kir6.2ΔCS-I154C + SUR1-GD, Kir6.2ΔCS + SUR1-GD, or Kir6.2ΔCS-T171C + SUR1-GD. The holding potential was -50 mV. The patch was excised into ATP-free solution at the arrows. ATP (10 mM, 1 mM, or 0.1 mM) was subsequently added to the intracellular solution as indicated. The dashed line indicates the zero current level.

rents (8, 18) such that coexpressed channels should only be sensitive to [ATP]. As shown in Fig. 4 and Table I, coexpression of SUR1-GD with Kir6.2ΔCS-I154C does not significantly alter the estimated $[ATP]_{sm}$ (1.4 ± 0.3 mM versus 1.8 ± 0.6 mM).

We also examined additional Kir6.2ΔCS mutants that displayed a range of ATP sensitivities. For each patch the membrane current before and immediately after excision was measured, and the ATP dose-response curve was then constructed. The K_i for ATP inhibition of Kir6.2ΔCS-I154C + SUR1-GD, Kir6.2ΔCS + SUR1-GD, and Kir6.2ΔCS-T171C + SUR1-GD currents were 0.49 ± 0.1 ($n = 14$), 0.78 ± 0.09 ($n = 29$), and 3.09 ± 0.49 mM ($n = 19$), respectively. As observed in the oocyte experiments, those channels that were least sensitive to ATP exhibited the largest currents in the cell-attached configuration and the smallest increment in current on patch excision (Fig. 3). The value of $[ATP]_{sm}$ estimated for the different K_{ATP} channel mutants varied between 1 and 1.8 mM (Fig. 4 and Table I), with an overall mean value of 1.36 ± 0.13 mM ($n = 66$). These values are somewhat lower than those found in oocytes, suggesting that $[ATP]_{sm}$ may be lower in COSm6 cells.

Effects of Metabolic Inhibition—In intact *Xenopus* oocytes, inhibition of cell metabolism by 3 mM azide leads to an increase in the whole-cell K_{ATP} current (15). Using the value for resting

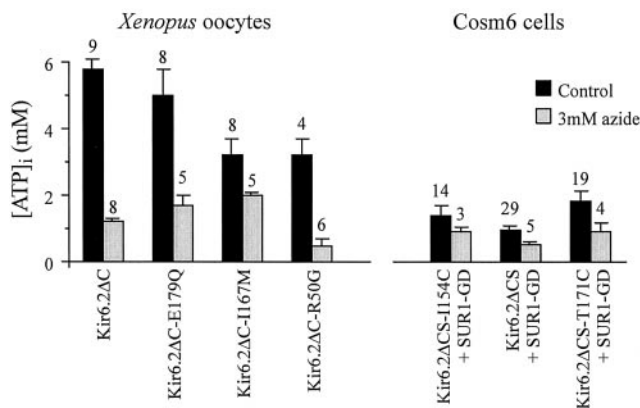


FIG. 4. Mean calculated ATP concentrations for oocytes (left) or COSM6 cells (right) expressing the indicated K_{ATP} channel constructs in the presence and absence of metabolic inhibitor. Black bars indicate the ATP concentration in control solution. Gray bars indicate the ATP concentration in the presence of the metabolic inhibitor azide (3 mM).

[ATP]_{sm} obtained above, we can estimate the fall in submembrane [ATP] following metabolic inhibition. Fig. 4 shows the estimated [ATP]_{sm} in the presence of 3 mM azide. The mean [ATP]_{sm}, calculated from all data, fell to 1.2 ± 0.1 mM ($n = 24$) when metabolism was inhibited. This value is similar to that measured biochemically for the bulk cytoplasm in the presence of 3 mM azide (1.7 mM, Ref. 15).

Submembrane [ATP] also fell in mammalian cells incubated in 3 mM azide (Fig. 4) to a mean value of 0.76 ± 0.11 mM ($n = 12$) after 10 min (averaged for all Kir6.2ΔCS mutants coexpressed with SUR1-GD). Even greater falls in [ATP]_{sm} were observed when cells were preincubated in the presence of 1 mM 2-deoxyglucose and 2.5 μg/ml oligomycin (Fig. 4); in this case, the mean value of [ATP]_{sm} was 0.1 ± 0.06 mM ($n = 5$) after a 30-min preincubation (measured for Kir6.2ΔCS mutants coexpressed with SUR1-GD). This is consistent with earlier studies that have shown that this protocol induces a marked activation of wild-type K_{ATP} channel activity, as measured by rubidium efflux (18).

DISCUSSION

It is implicit in the use of Kir6.2ΔC to measure [ATP]_{sm} that other cytosolic factors have little or no effect on channel activity or ATP sensitivity. Our results support this idea, because a similar estimate of [ATP]_{sm} is obtained for channels with different K_i for ATP inhibition. We have shown elsewhere that Kir6.2ΔC is selectively inhibited by ATP and is not substantially blocked by other nucleoside triphosphates ($K_i > 5$ mM, Ref. 17). Only ATP, Ap₄A ($K_i \approx 100$ μM), and ADP ($K_i \approx 250$ μM) were potent blockers of Kir6.2ΔC. The concentrations of Ap₄A and ADP in the bulk cytoplasm are believed to lie within the low and intermediate micromolar range, respectively (19, 20), and are much lower than that of ATP. Thus we assume that the activity of Kir6.2ΔC in the intact cell is largely determined by [ATP]_{sm}.

Recent studies have shown that the membrane phospholipid phosphatidylinositol bisphosphate decreases the sensitivity of the K_{ATP} channel to ATP and that the gradual loss of phosphatidylinositol bisphosphate from the membrane that occurs following patch excision is accompanied by an enhanced ATP sensitivity (21–23). Such a lowering of the K_i for ATP inhibition would lead to an underestimate of [ATP]_{sm}. Thus to avoid artifactual changes in ATP sensitivity, ATP dose-response curves were measured immediately after patch excision.

The mean value of the submembrane ATP concentration in oocytes (~5 mM) is approximately double that measured from the whole oocyte using a biochemical method (2.3 mM, Ref. 15). The difference may be only apparent and reflect exclusion of

ATP from certain compartments (such as the yolk platelets), or it may indicate an inverse ATP gradient between the membrane and bulk cytosol. We favor the former explanation because a similar difference was found in oocytes of the frog *Rana pipiens* in biochemical measurements of cytosolic (6 mM) and total (2.5 mM) [ATP] (24). Whatever the reason, our results do not support the widely held view that the submembrane ATP concentration is lower than that of the bulk cytosol (1–4).

Recently, the submembrane ATP concentration has been estimated in pancreatic β-cells using a membrane-tagged luciferin and found to be ~1 mM under resting conditions (3 mM glucose) (25). Our results on mammalian cells are in good agreement with these studies. Furthermore, the fact that two different methods provide a similar value for [ATP]_{sm} helps validate the different assumptions intrinsic to each method. The bulk cytosolic [ATP] in various mammalian cells is also ~1 mM: 1.0 mM in β-cells (25), 0.9 mM in HeLa cells (26), and 0.8–1.2 mM in COS-1 cells (27). The advantage of using Kir6.2ΔC as a biosensor is that it is able to respond very rapidly to changes in [ATP]_{sm}.

In conclusion, our results suggest that Kir6.2ΔC alone, or Kir6.2 coexpressed with a mutant SUR1, may be used as tools to monitor the submembrane ATP concentration in real time in a single cell. Inside-out patches excised from cells expressing mutant K_{ATP} channels might also be used to detect the local release of ATP from purinergic neurons, as described for acetylcholine release using acetylcholine receptor channels (28). In a similar fashion, inside-out macropatches containing mutant K_{ATP} channels might serve to monitor exocytosis from single secretory cells, as many types of secretory granules contain ATP. Importantly, our data also demonstrate that the submembrane ATP concentration lies in the millimolar, rather than the micromolar, range in both *Xenopus* oocytes and mammalian cells.

REFERENCES

- Ashcroft, F. M., and Ashcroft, S. J. H. (1990) *Cell. Signalling* **2**, 197–214
- Niki, I., Ashcroft, F. M., and Ashcroft, S. J. H. (1989) *FEBS Lett.* **257**, 361–364
- Aw, T. Y., and Jones, D. P. (1985) *Am. J. Physiol.* **249**, C385–C392
- Jones, D. P. (1985) *Am. J. Physiol.* **250**, C663–C675
- Proverbio, F., and Hoffman, J. F. (1977) *J. Gen. Physiol.* **69**, 605–632
- Prakriya, M., Solaro, C. R., and Lingle, C. J. (1996) *J. Neurosci.* **16**, 4344–4359
- Kakei, M., Kelly, R. P., Ashcroft, S. J. H., and Ashcroft, F. M. (1986) *FEBS Lett.* **208**, 63–66
- Nichols, C. G., Shyng, S. L., Nestorowicz, A., Glaser, B., Clement, J. P., IV, Gonzalez, G., Aguilar-Bryan, L., Permutt, M. A., and Bryan, J. (1996) *Science* **272**, 1785–1787
- Clement, J. P., IV, Kunjilwar, K., Gonzalez, G., Schwanstecher, M., Panten, U., Aguilar-Bryan, L., and Bryan, J. (1997) *Neuron* **18**, 827–838
- Shyng, S. L., and Nichols, C. G. (1997) *J. Gen. Physiol.* **110**, 655–664
- Inagaki, N., Gono, T., Clement, J. P., IV, Namba, N., Inazawa, J., Gonzalez, G., Aguilar-Bryan, L., Seino, S., and Bryan, J. (1995) *Science* **270**, 1166–1169
- Sakura, H., Ammälä, C., Smith, P. A., Gribble, F. M., and Ashcroft, F. M. (1995) *FEBS Lett.* **377**, 338–344
- Inagaki, N., Gono, T., Clement, J. P., IV, Wang, C. Z., Aguilar-Bryan, L., Bryan, J., and Seino, S. (1996) *Neuron* **16**, 1011–1017
- Tucker, S. J., Gribble, F. M., Zhao, C., Trapp, S., and Ashcroft, F. M. (1997) *Nature* **387**, 179–183
- Gribble, F. M., Ashfield, R., Ammälä, C., and Ashcroft, F. M. (1997) *J. Physiol.* **498**, 87–98
- Koster, J. C., Sha, Q., and Nichols, C. G. (1999) *J. Gen. Physiol.* **4**, 203–213
- Tucker, S. J., Gribble, F. M., Proks, P., Trapp, S., Ryder, T. J., Haug, T., Reimann, F., and Ashcroft, F. M. (1998) *EMBO J.* **17**, 3290–3296
- Shyng, S. L., Ferrigni, T., and Nichols, C. G. (1997) *J. Gen. Physiol.* **110**, 643–654
- Ripoll, C., Martin, F., Manuel-Rovira, J., Pintor, J., Miras-Portugal, M. T., and Soria, B. (1996) *Diabetes* **45**, 1431–1434
- Ghosh, A., Ronner, P., Cheong, E., Khalid, P., and Matschinsky, F. M. (1991) *J. Biol. Chem.* **266**, 22887–22892
- Fan, Z., and Makielski, J. C. (1997) *J. Biol. Chem.* **272**, 5388–5395
- Shyng, S.-L., and Nichols, C. G. (1998) *Science* **282**, 1138–1141
- Baukowitz, T., Schulte, U., Oliver, D., Herlitze, S., Krauter, T., Tucker, S. J., Ruppersberg, J. P., and Fakler, B. (1998) *Science* **282**, 1141–1144
- Miller, D. S., and Horowitz, S. B. (1986) *J. Biol. Chem.* **261**, 13911–13915
- Kennedy, H. J., Pouli, A. E., Ainscow, E. K., Jouaville, L. S., Rizzuto, R., and Rutter, G. A. (1999) *J. Biol. Chem.* **274**, 13281–13291
- Wang, R. H., Tao, L., Trumbore, M. W., Berger, S. L. (1997) *J. Biol. Chem.* **272**, 26405–26412
- Sippel, C. J., Dawson, P. A., Shen, T., and Perlmutter, D. H. (1997) *J. Biol. Chem.* **272**, 18290–18297
- Hume, R. I., Role, L. W., and Fischbach, G. D. (1983) *Nature* **305**, 632–634